

Experimental characterisation of digital Nyquist pulse-shaped dual-polarisation 16QAM WDM transmission and comparison with the Gaussian noise model of nonlinear propagation

Robert I. Killey¹, Robert Maher¹, Tianhua Xu¹, Lidia Galdino¹, Masaki Sato^{1,2}, Sean Kilmurray¹,
Benn C. Thomsen¹, and Polina Bayvel¹

1. *Optical Networks Group, Department of Electronic and Electrical Engineering, University College London, Torrington Place, London WC1E 7JE, UK, r.killey@ucl.ac.uk*

2. *NEC Corporation, Abiko, Japan*

ABSTRACT

We describe an experimental investigation of the performance of a DP-16QAM Nyquist WDM transmission system operating at 10 Gbaud with 10.01 GHz channel spacing, with an information spectral density (ISD) of 6.66 b/s/Hz (gross ISD of 8 b/s/Hz, with 20% FEC overhead). With seven WDM channels, the maximum transmission distance with BER < 1.5×10^{-2} over uncompensated standard single mode fibre with EDFA amplification was found to be 1940 km, similar to the value predicted by analytical calculation using the perturbative Gaussian noise model of nonlinear propagation.

Keywords: Nyquist WDM, fibre nonlinearity

1. INTRODUCTION

There is strong interest in optical signalling techniques which efficiently utilise the available optical bandwidth across the world's optical fibre networks. Spectral efficiency gains can be achieved by increasing the cardinality of the format and by reducing the channel spacing to values at, or approaching, the Nyquist limit, at which point the channel spacing is equal to the baud-rate. A key research question concerns the optimum signaling format to minimise inter-channel crosstalk at such low channel spacing, and to provide high tolerance to distorting effects such as dispersion and fibre nonlinearity [1]. A number of approaches are possible, including the use of orthogonal frequency division multiplexing (OFDM) [2], DFT-spread OFDM [3], all-optical OFDM [4] and single-carrier formats with Nyquist (sinc-like) pulse shaping [5]. In this paper, we focus on the digital Nyquist pulse shaping technique and describe recent work implementing a field programmable gate array (FPGA) and digital-to-analogue (DAC)-based transmitter for the characterization of dual polarization (DP) 16QAM Nyquist WDM systems. We describe back-to-back testing of the transmitter, and long-haul transmission experiments over uncompensated standard single mode fibre (SSMF) using a recirculating fibre loop, at a net information spectral density of 6.66 b/s/Hz. To assess the pulse shaping filter complexity required, a range of Nyquist filter roll-off factors were tested [6]. The experimental performance of the system was compared with results obtained using split-step Fourier algorithm based simulations, and the Gaussian noise model of nonlinear propagation.

2. NYQUIST-WDM TRANSCEIVER DESIGN

The experimental set-up of the 10 Gbaud Nyquist-WDM DP-16QAM transmitter is shown in Figure 1. An external cavity laser (ECL) with a linewidth of approximately 100 kHz was used as the seed for an optical comb generator (OCG), which used a Mach Zehnder modulator in series with a phase modulator, both overdriven with an amplified sinusoidal wave to generate seven wavelength channels with a spacing of 10.01 GHz. Odd and even channels were separated using three cascaded micro interferometer interleavers to allow decorrelated bit sequences to be encoded on neighbouring channels. Two pairs of Xilinx Virtex 5 FPGAs and Micram VEGA DACII digital-to-analog converters were used to generate the modulator drive waveforms. Linear driver amplifiers were used to boost the power of the drive signals. Anti-imaging filters were placed after the driver amplifiers to remove the images in the spectra resulting from the sample-and-hold operation of the DACs. The anti-imaging filters were 5th order Bessel filters with a 3-dB bandwidth of 7 GHz. The digital modulator drive waveforms were generated offline with Matlab as follows. Nyquist pulse shaping, root-raised-cosine (RRC) filters with roll-off factors of 0.1%, 1% and 10%, and pre-emphasis to compensate for the frequency response of the DACs, anti-imaging filters and modulators were applied to four de-correlated 2^{15} de Bruijn sequences, and the resulting waveforms were quantized to 6 bits and uploaded to memory in the FPGAs. After odd and even channels were separately modulated by IQ-MZMs, the two sets of channels were combined with a 3 dB optical coupler to form the 7 channel 10 GBaud Nyquist-16QAM signal with 10.01 GHz channel spacing. Next, polarization division multiplexing (PDM) was emulated by passing the signal through a polarization multiplexing stage. The optical spectrum of the resulting 7-channel signal (with the channel spacing adjusted to 11 GHz to allow the individual channels to be clearly seen) is shown in Figure 2.

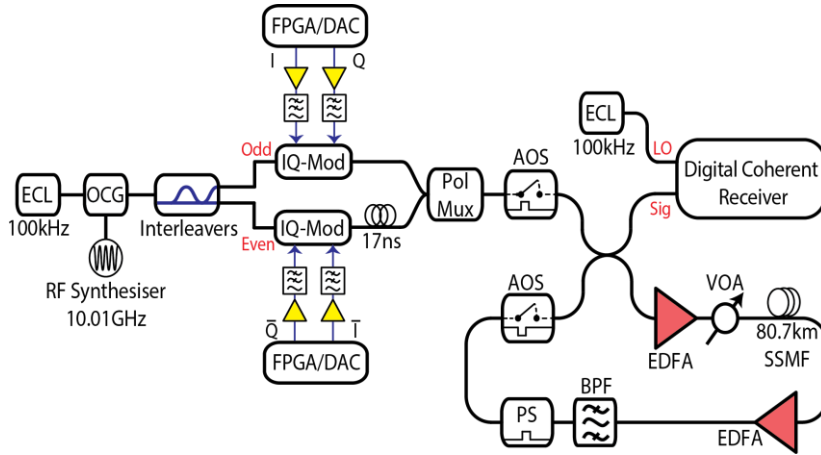


Figure 1. Experimental Nyquist-WDM DP-16QAM transmitter

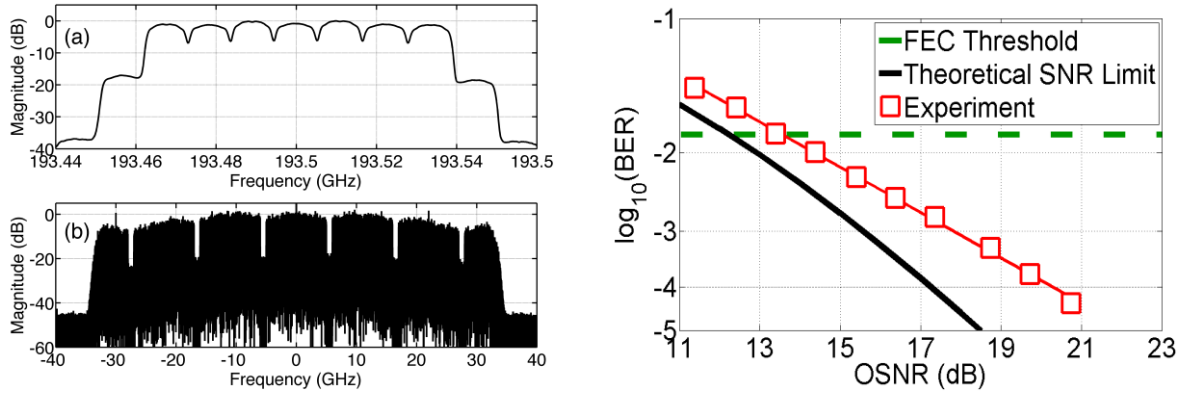


Figure 2. Left: (a) Optical spectrum of 7×10 GBaud Nyquist-WDM DP-16QAM. (b) Digital spectrum of the received signal. Right: Theoretical and measured back-to-back BER for 10 Gbaud Nyquist pulse-shaped DP-16QAM.

A polarization- and phase-diverse coherent receiver with a 3 dB electrical bandwidth of 24 GHz was used to receive the central of the seven channels. The incoming optical signal was combined with a free running local oscillator (LO), an ECL with 100 kHz linewidth, to generate signals proportional to in-phase and quadrature components of the two orthogonal polarizations. An 80 GSamples/s real time sampling oscilloscope with an analogue bandwidth of 30 GHz was used to digitise the signals, and subsequent digital signal processing (DSP) was carried out offline. The signal was downsampled to two samples per symbol, linear chromatic dispersion compensation was performed prior to the application of root-raised-cosine filters to achieve matched filtering. The signal was equalised using a 21-tap T/2-spaced radius directed equaliser (RDE) [7], with the constant modulus algorithm used for pre-convergence. The intermediate frequency offset was estimated and removed using the 4th order nonlinearity algorithm [8]. The carrier phase was estimated using a decision directed phase estimation algorithm and the complex field was averaged over a 64 T-spaced sliding window. Bit error ratio counting was performed on the central WDM channel.

Figure 2 shows the spectrum of the received digital signal prior to RRC filtering and downsampling, obtained using an FFT. Due to the relatively wide bandwidth of the photodetectors and ADCs, five Nyquist-WDM channels were detected simultaneously by a single receiver. The channel-of-interest (COI) at the LO wavelength is in the centre of the spectrum, with neighbouring channels to either side. The downsampling and RRC filtering removes the outer four channels, and only the centre channel (the COI) is processed.

3. BACK-TO-BACK TRANSCEIVER CHARACTERISATION

The transmitter performance was characterised in noise-loaded back-to-back tests. The output of an EDFA, generating wideband ASE noise, was passed through a variable optical attenuator before being combined with the signal, allowing the BER to be investigated at different OSNR values. BER versus OSNR was measured for single channel DP-16QAM with Nyquist pulse shaping with a RRC pulse shaping filter roll-off factor $\alpha = 0.1$ %. Figure 2 shows the resulting BER versus OSNR curves (measured with a 0.1 nm bandwidth), compared with the

theoretical curve. The implementation penalty was 1.3 dB at the FEC limit, assumed to be at a BER of 1.5×10^{-2} with 20% overhead.

4. TRANSMISSION EXPERIMENTS

A recirculating fibre loop, with the configuration shown in Figure 1, was used to assess the transmission performance of the 7-channel Nyquist-WDM signals over long-haul links. The power of the signal in the loop was maintained with a pair of EDFAs with a noise figure of 5 dB, and the launch power into the span was controlled using a variable optical attenuator (VOA). A tunable optical bandpass filter served the dual purpose of gain flattening and ASE filtering, A loop-synchronous polarisation scrambler (PS) was also included in the loop. The span comprised 80.7 km of standard SMF (G.652), and no inline dispersion compensation was used. Figure 3 plots the launch powers at which $\text{BER} = 1.5 \times 10^{-2}$ for the central of the seven Nyquist pulse shaped DP-16QAM modulated channels. The lower parts of the curves are limits due to ASE noise, while the upper parts arise from fibre nonlinearity. As can be seen in Figure 3, the numerical simulations (solid lines), which included the implementation penalty of the practical transceiver, predicted a maximum transmission distance of 2340km, at a launch power of -7 dBm per channel, when the RRC filter roll-off factor α was set at 0.1%. With the filter roll-off factor increased to 1%, the maximum reach reduced by 161km. The performance deteriorated sharply as the filter roll-off factor was increased further to 10%, with the system reach reducing to 890km, due to increased linear interchannel interference (ICI).

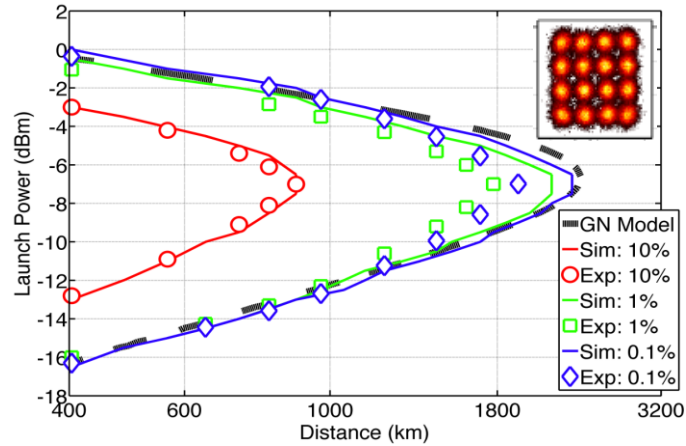


Figure 3. Signal launch power for $\text{BER} = 1.5 \times 10^{-2}$ versus transmission distance, for the central channel in 7-channel 10.01 GHz-spaced 10 Gbaud Nyquist WDM DP-16QAM transmission for pulse-shaping RRC filter roll-off factors $\alpha = 10\%$, 1% and 0.1%. Comparison of GN model results, split-step Fourier algorithm based simulation results and experimental measurements. Inset: Experimental X-polarisation constellation for $\alpha = 0.1\%$ at a transmission distance of 1940 km.

The experimental results (symbols) follow a similar trend in both the linear and nonlinear regions of the reach curve. A maximum transmission distance of 1940km was achieved when the roll-off factor was set at 0.1% and the optimal launch power was -7dBm, which is in good agreement with the simulations. The slight discrepancy in terms of maximum reach between the experimental points and the numerical simulation is attributed to polarization dependent loss (PDL), which occurs in a practical system but was not included in the simulations. A similar deterioration in transmission distance was experienced as the RRC filter roll-off factor was increased to 10%, with the reach reducing from 1940km to 888km.

5. COMPARISON WITH THEORY

To determine if the measured maximum transmission distance is similar to the theoretical prediction, we calculated the OSNR including terms for the linear amplified spontaneous emission (ASE) noise power and the nonlinear interference (NLI) noise power, for Nyquist-spaced WDM transmission with the same signal optical bandwidth as used in the experiments, and with the link configuration that was used in the recirculating loop. The following equation was used to calculate OSNR [9]:

$$(1)$$

$$\text{OSNR} = \frac{P_{TX, ch}}{P_{ASE} + P_{NLI}}$$

where $P_{TX, ch}$ is the launch power per WDM channel, and P_{ASE} and P_{NLI} are, respectively, the amplified spontaneous emission noise power, and the nonlinear interference noise power in a 0.1 nm ($\Delta\nu = 12.5$ GHz) bandwidth. Expressions for the power spectral density (PSD) of the FWM-induced noise in Nyquist-limited WDM transmission are derived in [9]-[11]. The expression below gives the NLI noise PSD [9]:

$$I_{NLI} = \left(\frac{2}{3}\right)^3 N_S \gamma^2 L_{eff} \frac{\ln(\pi^2 |\beta_2| L_{eff} B^2)}{\pi |\beta_2|} I_{Tx}^3 \quad (2)$$

where $I_{Tx} = P_{Tx, ch}/\Delta f$ is the signal PSD (Δf is the WDM channel spacing), $\gamma = 1.2 \text{ W}^{-1} \text{ km}^{-1}$ is the fibre nonlinear coefficient, the nonlinear effective length $L_{eff} = 21$ km, $\beta_2 = -21.7 \text{ ps}^2 \text{ km}^{-1}$ is the fibre group velocity dispersion, and the optical bandwidth of the signal $B = 70.1$ GHz. The resulting FWM-induced noise power, $P_{NLI} = I_{NLI} \Delta\nu$ is added to the ASE noise power, calculated using the EDFA noise figure of 5 dB, to obtain the OSNR, which, from the back-to-back BER curve in Figure 2, is used to calculate bit error ratio. The results obtained with the GN model are plotted in Figure 3 (dashed line). Good agreement between theoretically predicted and experimentally measured transmission distances (with RRC filter roll-off factor of 0.1%) was found.

6. CONCLUSIONS

We described an experimental evaluation of a Nyquist-WDM transmission system. A transmitter was implemented based on field programmable gate arrays (FPGAs) and digital-to-analogue converters (DACs), and an optical comb generator. We used the system to generate and characterise seven 10.01 GHz-spaced WDM channels, with single-carrier 10 Gbaud dual-polarisation 16QAM signal format with digital Nyquist pulse-shaping. We firstly assessed back-to-back performance, measuring an implementation penalty of 1.3 dB in the required OSNR at $\text{BER} = 1.5 \times 10^{-2}$, and, secondly, performed long-haul transmission experiments using a recirculating fibre loop. The impact of varying the roll-off parameter, α , of the root raised cosine pulse shaping filters on the interchannel interference, and hence the maximum transmission distance, was investigated. The experimental results were compared with values predicted by the theoretical models of linear and nonlinear noise. The maximum transmission distance of 1940 km with $\alpha = 0.1\%$ was similar to the value predicted using the Gaussian-noise model of nonlinear propagation.

ACKNOWLEDGEMENTS

The work was funded by the UK EPSRC Programme Grant UNLOC (Unlocking the capacity of optical communications) EP/J017582/1, the EU FP7 project ASTRON, the EPSRC grant COSINE EP/I012702/1, and Huawei Technologies. Lidia Galdino is supported by CNPq-Brasil and Sean Kilmurray is supported by the EPSRC UCL-Cambridge Centre for Doctoral Training in Photonic Systems Development.

REFERENCES

- [1] R.-J. Essiambre *et al.*, *J. Lightwave Technol.* 28, 4 (2010), pp. 662-701.
- [2] W. Shieh *et al.*, *Opt. Exp.* 16, 2 (2008), pp. 841-859.
- [3] Y. Tang *et al.*, *IEEE Photon. Technol. Lett.* 22, 16 (2010), pp. 1250-1252.
- [4] A. Sano *et al.*, in *Proc. ECOC 2007*, 2007.
- [5] G. Bosco *et al.*, *J. Lightwave Technol.* 29, 1 (2011), pp. 53-61.
- [6] R. Schmogrow *et al.*, *Opt. Exp.* 20, 26 (2012), pp. B543-B551.
- [7] M. J. Ready and R. P. Gooch, *Int. Conf. on Acoustics, Speech, and Signal Processing (ICASSP)*, D11.16 (1990).
- [8] S. J. Savory *et al.*, *Opt. Exp.* 15, 5 (2007), pp. 2120-2126.
- [9] P. Poggiolini *et al.*, *IEEE Photon. Technol. Lett.* 23, 11 (2011), pp. 742-744.
- [10] A. Splett *et al.*, in *Proc. ECOC 1993*, 1993, vol. 2, pp. 41-44.
- [11] P. Poggiolini, *J. Lightwave Technol.* 30, 24 (2012), pp. 3857-3879.